Solid-State NMR Analysis Comparing the Designer-Made Antibiotic MSI-103 with Its Parent Peptide PGLa in Lipid Bilayers†

Erik Strandberg,‡ Nathalie Kanithasen,§ Deniz Tiltak,§ Jochen Bürck,‡ Parvesh Wadhwani,‡ Olaf Zwernemann,‡ and Anne S. Ulrich*,‡,§

Institute of Biological Interfaces, Forschungszentrum Karlsruhe, P.O. Box 3640, 76021 Karlsruhe, Germany, and Institute of Organic Chemistry, University of Karlsruhe, Fritz-Haber-Weg 6, 76131 Karlsruhe, Germany

Received September 25, 2007; Revised Manuscript Received December 17, 2007

ABSTRACT: The amphiphilic α-helical peptide $(KIAGKIA)_3$-NH_2 (MSI-103) is a designer-made antibiotic, based on the natural sequence of PGLa from *Xenopus laevis*. Here, we have characterized the concentration-dependent alignment and dynamic behavior of MSI-103 in lipid membranes by solid-state ^2H and ^{19}F NMR, using orientational constraints from seven Ala-d_3-labeled analogues and five 4-CF_3-phenylglycine labels. As previously found for PGLa, MSI-103, too, assumes a flat surface-bound S-state alignment at low peptide concentrations, and it also realigns to a tilted T-state at higher concentrations. For PGLa, the stability of the T-state had been attributed to the specific assembly of antiparallel dimers; hence, it is remarkable that the artificial KIAGKIA repeat sequence can also dimerize in the same way in liquid crystalline lipid bilayers. Oriented circular dichroism analysis shows that for MSI-103 the threshold for realignment from the S-state to the T-state is ∼3-fold lower than for PGLa (at a peptide-to-lipid ratio of 1:240 in dimyristoylphosphatidylcholine, compared to 1:80). Furthermore, MSI-103 becomes laterally immobilized in the lipid bilayer at a concentration ratio of 1:50, which occurs for PGLa only above 1:20. The superior antimicrobial activity of MSI-103 over PGLa thus appears to correlate with its stronger tendency to realign and self-assemble. The hemolytic activities of MSI-103 and its analogues, on the other hand, are shown here to correlate purely with the respective changes in hydrophobicity.

Many species, from prokaryotes to humans, use antimicrobial peptides as a first line of defense against bacteria (*1*−*5*). There is much interest in the detailed functional mechanisms of these peptides, which have very heterogeneous primary structures but similar effects. Many of them are cationic and form amphipathic α-helices when bound to lipid membranes, for example, the magainin family of peptides found in the skin of the African frog *Xenopus laevis* (*6*). For magainin, it was shown that the all-D form has the same biological activity as the normal L-peptide, which indicates that no chiral receptor is involved (*7*). It thus seems likely that the peptides bind to the bacterial membranes, disrupt their function, and kill the microorganism (*1*). The positive charge confers them with a high selectivity, since bacterial membranes contain many negatively charged lipids, which do not usually occur in the outer leaflet of eukaryotic plasma membranes.

PGLa[1] ("peptidyl-glycylleucine-carboxyamide") belongs to the magainin family of peptides and shows a strong antimicrobial activity and high selectivity against bacteria (*8*−*10*). Its conformation has been described by CD and liquid-state NMR as a random coil in aqueous solution, but as an α-helix in the presence of lipids (*11*−*14*). Helical wheel projections of PGLa and MSI-103 are shown in Figure 1. Solid-state NMR has been extensively used to study PGLa in lipid membranes, as this technique is well-suited to determining the conformation, alignment, and dynamic behavior of membrane-active peptides with quasi-atomic resolution (*15*, *16*). By ^2H, ^{15}N, and ^{19}F NMR, we have recently demonstrated that PGLa changes its orientation in lipid bilayers in a concentration-dependent manner. Above a certain threshold, it realigns from an "S-state", where the helix is aligned parallel to the membrane surface, to a tilted "T-state" with an oblique peptide orientation (*13*, *17*, *18*). The stability of the unusual tilt angle was attributed to the proposed formation of antiparallel peptide dimers at high concentrations, as it is known that magainin and its relatives have a tendency to dimerize (*19*−*21*). A more detailed ^2H NMR study showed that the presence of charged lipids and the degree of sample hydration also had an influence on the equilibrium among the free peptide, the S-state, and the T-state (*22*). Interestingly, when PGLa was mixed with magainin 2 in an equimolar ratio, it assumed an almost upright helix orientation in the lipid bilayer, representing an

† This research was funded by the DFG-Center for Functional Nanostructures (E1.2).

* To whom correspondence should be addressed. E-mail: anne.ulrich@ibg.fzk.de.

‡ Forschungszentrum Karlsruhe.

§ University of Karlsruhe.

[1] Abbreviations: Ala-d_3, [3,3,3-$^2H_3$]-L-alanine; CD, circular dichroism; CF_3-Bpg, 4-CF_3-bicyclopentylglycine; CF_3-Phg, 4-CF_3-phenylglycine; DMPC, dimyristoylphosphatidylcholine; DMPG, dimyristoylphosphatidylglycerol; MIC, minimal inhibitory concentration; MLV, multilamellar vesicle; MSI-103, peptide $(KIAGKIA)_3$-NH_2; OCD, oriented circular dichroism; P:L, peptide-to-lipid molar ratio; PGLa, peptide GMASKAGAIAGKIAKVALKAL-NH_2; ρ, azimuthal rotation angle; rmsd, root-mean-square deviation; S_{mol}, molecular order parameter; τ, tilt angle; TFE, trifluoroethanol.

10.1021/bi701944r CCC: $40.75
Published on Web 01/26/2008

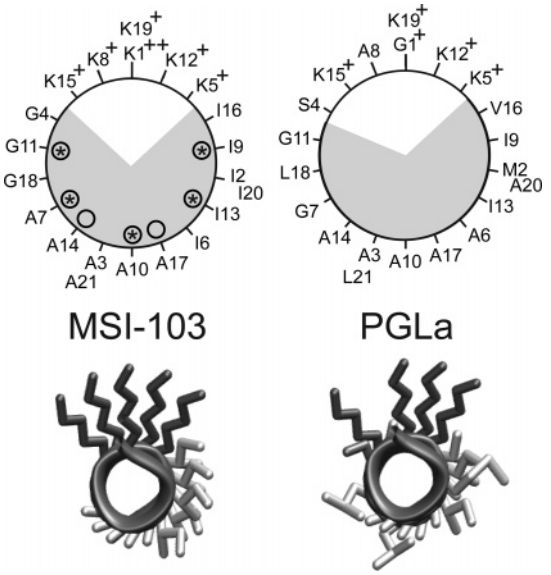

FIGURE 1: Helical wheel representation of the amphiphilic peptides MSI-103 and PGLa. The hydrophobic sector of the peptide is shaded, and the charged lysines and N-terminus are marked with a plus. The positions in MSI-103 labeled with Ala-d_3 are marked with circles, and positions labeled with CF_3-Phg are indicated with stars. In the bottom panel, an end view of each helix is shown with the amino acid side chains in stick representation.

inserted "I-state" (*23*). In this transmembrane alignment, it seems that PGLa−magainin 2 heterodimers are formed, which may further assemble as a toroidal pore in the membrane. These NMR results can explain the previously observed synergistic antimicrobial effect between PGLa and magainin 2, both of which are simultaneously present in the frog skin.

Here, we have used solid-state ^{19}F and ^{2}H NMR for an analogous structure analysis of the designer-made antimicrobial peptide MSI-103, the sequence of which is derived from PGLa (*3*). The main modification is a replacement of Gly1 and Ala8 with charged Lys residues, which increases the charge and the amphiphilic moment of the peptide (see Table 1 and Figure 1), two properties proposed to be important for antimicrobial activity (*3*, *24*). With the generalized heptameric repeat $(KxxxKxx)_n$ as a basic pattern, combinations with different amino acids were synthesized and tested. The trimeric motif $(KIAGKIA)_3$-NH_2 exhibited the highest antimicrobial activity and is called MSI-103 (*3*). Like PGLa, MSI-103 was also seen by CD to change from a random coil in solution to an α-helix in the presence of lipid vesicles (*25*) and to induce leakage of vesicles. It exhibited a 4−8 times lower minimum inhibitory concentration (MIC) than PGLa against three bacterial strains that were tested (*3*, *25*), but also a higher hemolytic activity (*25*). In a recent study, we found a slightly higher antimicrobial activity for MSI-103 than for PGLa against some different bacterial strains, and a hemolytic activity similar to that for PGLa (*26*).

MSI-103 has been previously investigated by solid-state NMR (under the name of "K3") in lipid systems that were either frozen or lyophilized (*20*, *21*). Chemical shifts and distances were measured in isotope-labeled peptides using MAS and REDOR experiments, which confirmed the α-helical conformation and suggested the formation of parallel dimers that remained in contact with the phospholipid headgroups. The REDOR data suggested the simultaneous presence of monomeric and dimeric peptides forming a pore, though the orientation of the helices in the membrane was not accessible from these distance measurements. Initial ^{19}F NMR experiments with a 3F-Ala-labeled analogue in oriented NMR samples suggested that MSI-103 is able to change its membrane alignment in a concentration-dependent manner, but a quantitative analysis had not been possible with this single ^{19}F label (*21*).

Table 1: Amino Acid Sequences of the Peptides Used

Peptide	Labeled position	Sequence
PGLa wt	None	GMASKAGA**IAGKIAK**VALKAL-NH_2
MSI-103 wt	None	KIAGKIAK**IAGKIAK**IAGKIA-NH_2
MSI-A7-^{19}F	Ala7 by CF_3-Phg	KIAGKI-CF_3-Phg-KIAGKIAKIAGKIA-NH_2
MSI-I9-^{19}F	Ile9 by CF_3-Phg	KIAGKIAK-CF_3-Phg-AGKIAKIAGKIA-NH_2
MSI-A10-^{19}F	Ala10 by CF_3-Phg	KIAGKIAKI-CF_3-Phg-GKIAKIAGKIA-NH_2
MSI-G11-^{19}F	Gly11 by CF_3-Phg	KIAGKIAKIA-CF_3-Phg-KIAKIAGKIA-NH_2
MSI-I13-^{19}F	Ile13 by CF_3-Phg	KIAGKIAKIAGK-CF_3-Phg-AKIAGKIA-NH_2
MSI-A7-^{2}H	Ala7 by Ala-d_3[a]	KIAGKI-Ala-d_3-KIAGKIAKIAGKIA-NH_2
MSI-I9-^{2}H	Ile9 by Ala-d_3	KIAGKIAK-Ala-d_3-AGKIAKIAGKIA-NH_2
MSI-A10-^{2}H	Ala10 by Ala-d_3[a]	KIAGKIAKI-Ala-d_3-GKIAKIAGKIA-NH_2
MSI-G11-^{2}H	Gly11 by Ala-d_3	KIAGKIAKIA-Ala-d_3-KIAKIAGKIA-NH_2
MSI-I13-^{2}H	Ile13 by Ala-d_3	KIAGKIAKIAGK-Ala-d_3-AKIAGKIA-NH_2
MSI-A14-^{2}H	Ala14 by Ala-d_3[a]	KIAGKIAKIAGKI-Ala-d_3-KIAGKIA-NH_2
MSI-A17-^{2}H	Ala17 by Ala-d_3[a]	KIAGKIAKIAGKIAKI-Ala-d_3-GKIA-NH_2

[a] Nonperturbing labels.

Here, we have acquired a large number of orientational constraints from a series of selectively ^{19}F- and ^{2}H-labeled peptides to determine the concentration-dependent alignment and mobility of MSI-103 in lipid bilayers. In this solid-state NMR study, all samples are in the liquid crystalline state, which is biologically more relevant than a frozen or lyophilized system. As a model membrane, we focus on DMPC and also include a DMPC/DMPG mixture to imitate the negative charge of bacterial membranes. The conformation, alignment, and dynamic behavior of MSI-103 can thus be compared with our previous NMR results for PGLa in the same environments. Oriented CD is introduced here as a method complementary to NMR, for determining the threshold of realignment more accurately. Specifically, we were interested in determining whether and at which concentration MSI-103 can realign from an S-state to a T-state or I-state. Whether the artificial KIAGKIA repeat sequence can dimerize in a fashion similar to that of the natural peptide PGLa is also intriguing. After all, it may be expected that specific dimerization interfaces have evolved such that PGLa can function optimally, both as a homodimer on its own and as a heterodimer in synergy with magainin 2. If we compare the two peptides PGLa and MSI-103 in terms of their respective antimicrobial and hemolytic activities, any similarities and differences must be related to the subtle differences in their primary sequences and can then hopefully be interpreted in light of the structural NMR and CD results. Ultimately, the aim of this study is to identify specific physicochemical parameters that correlate with the

antimicrobial function or hemolytic side effects, which will allow us to predict and improve the therapeutic potential of new peptide sequences.

MATERIALS AND METHODS

Materials. Dimyristoylphosphatidylcholine (DMPC) and dimyristoylphosphatidylglycerol (DMPG) were purchased from Avanti Polar Lipids (Alabaster, AL), and deuterium-depleted water was from Acros (Schwerte, Germany) and Sigma-Aldrich (Taufkirchen, Germany). MSI-103 was labeled at seven different positions with Ala-d_3 (from Cambridge Isotope Laboratories, Andover, MA) and at five positions with 4-CF_3-Phg (from ABCR, Karlsruhe, Germany), replacing Ala, Gly, or Ile (Table 1). All peptides were synthesized using standard Fmoc protocols, purified by HPLC, and identified by MALDI, as previously reported in detail (*13*, *27*). The ^{19}F-labeled peptides were synthesized using a mixture of L- and D-CF_3-Phg, and the peptide with the L-amino acid was identified as previously described (*27*) to be used in the NMR experiments. In an attempt to synthesize a sixth analogue with L-CF_3-Phg at the Ala14 position, the L- and D-epimeric peptides could not be separated by HPLC; hence, this labeled site was not included in the analysis.

Biological Tests. Antimicrobial assays and hemolysis tests were performed on the mutated peptide analogues to check whether they were still biologically active, as described previously (*26*). Antimicrobial activity was measured by a standard minimal inhibitory concentration (MIC) assay, carried out with Gram-positive *Bacillus subtilis* (ATCC 6633) and *Micrococcus luteus* (DSM 1790) and with Gram-negative *Escherichia coli* (DH5α) and *Acinetobacter* sp (DSM 586). Hemolytic activity was examined with a serial 2-fold dilution assay, by incubating erythrocytes with peptide solutions at 37 °C for 20 min with gentle shaking. The tubes were centrifuged at 20000*g* for 5 min to pellet the cells, and the absorbance at 540 nm was recorded against water. The percentage lysis was then calculated relative to 0% lysis with buffer and 100% lysis by Triton X-100. The absorbance measurement was repeated three times, and the averaged values were used.

Circular Dichroism Spectroscopy. CD spectra were recorded on a Jasco J-810 spectropolarimeter (Jasco Co., Tokyo, Japan), as reported previously (*13*). The peptides were measured at 20 °C in 10 mM sodium phosphate buffer (pH 7.0) containing 50% (v/v) trifluoroethanol (TFE) and averaged 3-fold, and an averaged baseline of the pure solvent mixture was subtracted. Due to the difficulty in accurately determining the absolute peptide concentrations, the spectra were normalized to the ellipticity of the wild-type peptide at 191 nm, with the intention of emphasizing any changes in the line shape.

The home-built setup used for the oriented CD (OCD) measurements is described in detail elsewhere (*28*, *29*). The macroscopically oriented multilayered peptide/lipid samples for the OCD measurements were prepared as described previously (*30*), following the same protocol as for oriented NMR samples below. Briefly, for OCD, ≤0.2 mg of lipid and the appropriate amount of peptide were deposited on a quartz window (patch ∼10 mm in diameter) from a 1:1 mixture of chloroform and methanol. After evaporation of the solvent, the sample was further dried under vacuum for 3 h. The window was assembled in the OCD cell and hydrated for ∼15 h at 30 °C and 97% relative humidity using a saturated K_2SO_4 solution.

NMR Spectroscopy. Oriented and nonoriented samples for solid-state NMR were prepared as previously described (*18*), following a procedure similar to that used for OCD. For nonoriented multilamellar vesicle (MLV) ^{2}H NMR samples we used 2 mg of peptide, for oriented ^{2}H NMR samples 1.2−2.0 mg of Ala-d_3-labeled peptides, and for oriented ^{19}F NMR samples 0.15−2.0 mg of CF_3-Phg-labeled peptides. The respective amount of lipid was calculated to give the desired peptide-to-lipid molar ratio (P:L).

All NMR measurements were carried out on a Bruker Avance 500 or 600 MHz spectrometer (Bruker Biospin, Karlsruhe, Germany) at 308 K. ^{31}P NMR was used to check the quality of the lipid orientation in the samples, using a Hahn echo sequence with phase cycling (*31*). ^{2}H NMR experiments were performed using a quadrupole echo sequence (*32*) with a 4.5 μs 90° pulse, an echo delay of 30 μs, a 80 ms relaxation delay time, a 250 kHz spectral width, and 2048 data points. Between 100 000 and 1 000 000 scans were collected and processed by zero filling to 16 384 data points and a 400 Hz exponential multiplication, followed by Fourier transformation. ^{19}F NMR experiments were performed with an antiringing sequence to reduce background signals from the probe (*33*), using a 2.0 μs 90° pulse, a 1 s relaxation delay time, a 500 kHz spectral width, 2048 data points, and proton decoupling with a ttpm20 sequence (*34*). Between 2000 and 10 000 scans were collected; the data were processed by zero filling to 4096 data points and a 200 Hz exponential multiplication, followed by Fourier transformation. Spectra were referenced to a 100 mM NaF solution for which the ^{19}F signal was set to −119.5 ppm.

Structure Calculations. The alignment and dynamics of a rigid peptide in the membrane can be described by three parameters, namely, the tilt angle τ of the dominant symmetry axis with respect to the bilayer normal, the azimuthal rotation angle ρ around this axis, and the molecular order parameter S_{mol}. Several different membrane-bound peptides have been characterized this way (*13*, *16*−*18*, *22*, *23*, *27*, *35*−*40*). Given that the effective quadrupolar/dipolar tensor is collinear with the C-CD_3/C-CF_3 axis of a ^{2}H-labeled/^{19}F-labeled peptide, at least three orientational constraints are required to determine τ, ρ, and S_{mol}. In practice, more than three are needed, especially for ^{2}H NMR where the sign of the quadrupole splitting is not accessible (*41*−*44*). In a rapidly rotating CF_3 group, the sign of the dipolar splitting is evident from the one-pulse spectrum, and typically four orientational constraints are sufficient (*13*, *38*, *40*).

To calculate orientational constraints from the NMR data, a quadrupole coupling constant (e^2qQ/h) of 167 kHz for an aliphatic C−D bond was used, giving a maximum quadrupolar splitting of 84 kHz for the Ala-d_3 labels (*45*), and a maximum ^{19}F dipolar splitting of 15.8 kHz was taken for CF_3-Phg (*13*). The peptide MSI-103 was modeled as an ideal helix, the alignment of which was fitted to the orientational constraints. In this molecular frame, the tilt τ defines the angle between the helix axis (N- to C-terminus) and the bilayer normal. The azimuthal angle ρ is defined as a right-handed rotation around the helix axis, with $\rho = 0°$ being defined as the orientation when the vector projecting radially

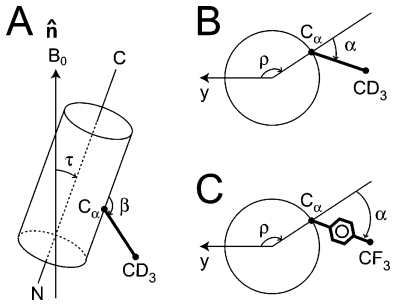

FIGURE 2: Definition of angles used in the calculations. (A) The helix tilt angle τ is the angle between the peptide axis (from N- to C-terminus) and the bilayer normal $\hat{\mathbf{n}}$ which is usually aligned parallel to the magnetic field direction B_0. For $\tau = 0°$, the helix would be oriented along $\hat{\mathbf{n}}$. The angle β fixes the $C^\alpha-CD_3$ bond vector relative to the helix axis. (B) View perpendicular to the helix, with the C-terminal direction out of the paper. The azimuthal rotation of the peptide is defined by the angle ρ. For $\rho = 0°$, the radial vector from the helix center through the C^α atom of residue Lys12 would be aligned with the *y*-axis, which is parallel to the membrane surface. The projection of the $C^\alpha-CD_3$ bond vector onto the plane perpendicular to the helix axis is fixed by the angle α. (C) Equivalent definitions for the CF_3-Phg side chain.

through the C^α atom of Lys12 is aligned parallel to the membrane plane, as illustrated in Figure 2. The orientation of the $C^\alpha-C^\beta$ bond in the molecular frame is described by an angle β between the bond vector and the helix axis. The angle α is defined by the vector radiating from the helix axis through the C^α atom and by the projection of the $C^\alpha-C^\beta$ bond vector onto a plane perpendicular to the helix. In the same plane, the rotational angle between two consecutive amino acids along the helix is called ω. For the Ala-d_3 labels, we described an α-helix (model A) using a β of 121.1°, an α of 53.2°, and an ω of 100°, as deduced from an α-helical polyalanine model constructed in SYBYL using a φ of −58° and a ψ of −47° (*13*). To investigate the possibility that the peptide might form other helical structures, the parameters corresponding to an ideal 3_{10}-helix ($\beta = 111.2°$, $\alpha = 53.5°$, and $\omega = 119°$) and π-helix ($\beta = 131.1°$, $\alpha = 52.5°$, and $\omega = 85.3°$) also were tested (*13*). For the CF_3-Phg labels, a different α-helical side chain geometry (model B) was also used, in which $\beta = 110°$, $\alpha = 47°$, and $\omega = 100°$ (*13*). This model had been proposed on the basis of an energy-minimized α-helix and was previously found to fit better than the ideal α-helix to the ^{19}F NMR data of PGLa labeled with CF_3-Phg and CF_3-Bpg (*13*, *40*).

To take motional averaging into account in the analysis, a third parameter is introduced, namely, a simplified order parameter, S_{mol}, which describes global wobbling motions of the peptide. Its effect in our calculations is to reduce all splittings by a constant factor between 1.0 and zero, corresponding to a uniaxial ordering tensor. In a grid search for the best-fit peptide structure, the helix is systematically rotated, and the theoretical quadrupole splittings are calculated for different combinations of τ, ρ, and S_{mol}. The parameters τ and ρ are changed in steps of 1° from 0 to 180°, and S_{mol} is changed in steps of 0.01 from 0 to 1, to find the parameters giving the lowest root-mean-square deviation (rmsd) with respect to the experimental data. The meaning of the rmsd is interpreted the following way: The experimental error in our quadrupole splittings was estimated to be no more than 1 kHz, which was found by repeated measurements on a sample or by use of duplicate samples.

Table 2: Antimicrobial Activity of the Peptides

	minimum inhibitory concentration (μg/mL)			
	Gram-negative		Gram-positive	
peptide	*E. coli* (D5α)	*Acinetobacther* sp (DSM 586)	*B. subtilis* (ATCC 6633)	*M. luteus* (DSM 1790)
PGLa wt[a]	8	8	4	4
MSI-103 wt[a]	4	8	8	8
MSI-A7-^{19}F	8	16	8	8
MSI-I9-^{19}F	8	8	8	4
MSI-A10-^{19}F	8	32	8	4
MSI-G11-^{19}F	32	128	32	8
MSI-I13-^{19}F	8	8	8	4
MSI-I9-^{2}H	8	8	32	8
MSI-G11-^{2}H	8	8	8	4
MSI-I13-^{2}H	16	8	8	16

[a] From ref *26*.

All rmsd values below this must be called "good" fits. It should be noted that our structural model is based on the assumption of an ideal α-helical structure. Slight deviations are expected for amphiphilic peptides; hence, even larger rmsd values may be acceptable. In a previous study on uniformly hydrophobic transmembrane model peptides, the fit to an ideal α-helix had been justified by the very small rmsd values of typically less than 1 kHz (*36*, *38*). Here, we estimate that for MSI-103 at 1:200 the intrinsic error in τ and ρ is approximately ±3°, according to the area in the error plot covering a rmsd of 1 kHz around the best fit. When the ^{2}H and ^{19}F NMR data are compared, the maximum value of the respective interaction should be taken into account, which is 84 kHz for Ala-d_3 and 15.8 kHz for CF_3-Phg, the latter being a factor of 5.3 lower. Thus, a rmsd of 1.0 kHz for a ^{2}H fit is comparable with a rmsd of 0.2 kHz for a ^{19}F fit.

RESULTS

Biological Activities of the Labeled MSI-103 Analogues. For solid-state NMR structure analysis, a series of 12 MSI-103 analogues (see Table 1) were synthesized with single Ala-d_3 or CF_3-Phg labels. Except for the entirely nonperturbing substitutions of a native Ala residue with Ala-d_3, the other labeled peptides contain one amino acid that differs from the wild-type MSI-103 sequence. To check whether these mutations have any effect on the antimicrobial activity, minimum inhibitory concentrations (MICs) were determined for wild-type MSI-103 and its analogues. Table 2 shows that the antimicrobial activities are almost the same, except for that of MSI-G11-^{19}F, which had a considerably lower activity against most bacterial strains that were tested. It can therefore be expected that the functionally relevant membrane interactions of the labeled peptides are the same as for the wild-type MSI-103, expect for the analogue in which Gly11 was replaced with CF_3-Phg.

In view of its therapeutic potential as a drug, it is also important to assess the hemolytic side effects of MSI-103 and the labeled analogues. It is seen in Table 3 that the hemolytic activity was much more sensitive to small changes in the primary sequence than the antimicrobial activity. When Ile9 or Ile13 was replaced with the less hydrophobic Ala-d_3, the hemolytic activity was almost completely abolished, whereas replacing Gly7 with the more hydrophobic Ala-d_3 induced a higher activity. When Ile9 or Ile13 was replaced

Table 3: Hemolytic Activity of the Peptides

	% hemolysis			
peptide	125 μg/mL	250 μg/mL	500 μg/mL	1000 μg/mL
PGLa wt	1	3	18	86
MSI-103 wt	9	24	45	76
MSI-A7-^{19}F	21	39	86	92
MSI-I9-^{19}F	4	15	30	51
MSI-A10-^{19}F	71	97	102	101
MSI-G11-^{19}F	78	89	96	95
MSI-I13-^{19}F	4	9	21	48
MSI-I9-^{2}H	−1	2	1	3
MSI-G11-^{2}H	26	43	81	96
MSI-I13-^{2}H	1	0	0	4

with CF_3-Phg, the hemolytic activity was slightly reduced compared to that of the wild-type peptide, but when Ala10 or Gly11 was replaced with the hydrophobic CF_3-Phg, a much higher activity was observed. It should be noted that typical MIC values were around 8 mg/mL, while hemolysis was usually still weak even up to 125 mg/mL; therefore, different mechanisms are likely to cause these distinct biological effects. The large difference in concentration needed to kill bacteria and to lyse erythrocytes is a measure of the selectivity of the peptides; hence, MSI-103 is a good drug candidate with a high therapeutic index (*3*, *25*, *26*).

Conformation and Helix Alignment by CD. The conformation of MSI-103 was examined by circular dichroism in a membrane-mimicking environment to check whether any of the ^{2}H or ^{19}F labels had a perturbing effect of the conformation of the helix. Figure 3 shows the CD spectra of the wild-type peptides and mutated MSI-103 analogues in a TFE/buffer solution (1:1, v/v). It is seen that all peptides are predominantly α-helical, and within the intrinsic error of the determination of the peptide concentration, no change in the secondary structure is found for any of the labeled analogues.

Oriented circular dichroism (OCD) is well suited to studying the membrane-bound α-helical peptides, as it can be used to determine the approximate helix tilt angle (*28*, *29*, *46*, *47*). This sensitive method does not require any labeling and is perfectly complementary to solid-state NMR, as it uses the same kind of macroscopically aligned membrane samples. We collected OCD spectra of MSI-103 in DMPC over a wide range of different peptide-to-lipid ratios from 1:400 to 1:20 (see Figure 4A). The line shapes at low concentrations closely resemble the OCD spectra of PGLa and related peptides in their surface-bound S-state, while at high concentrations, the spectra indicate a tilted T-state (*28*, *29*, *48*). On the basis of the pure S- and T-state spectra at the most extreme concentrations (1:400 and 1:20), all other line shapes at intermediate concentrations could be deconvoluted into their two respective contributions. That way it was possible to quantify the relative amount of S- and T-states and to determine the threshold concentration for the realignment (see Figure 4B). This threshold is defined as the lowest concentration for which a tilted state starts to appear, which is found to be at a P:L of 1:240 for MSI-103 in DMPC. In the same system, all peptides have then finally reached the T-state at 1:60. For comparison, the same analysis of PGLa under the same conditions in DMPC had given a threshold of 1:80, with all peptides reaching the T-state at 1:20 (*28*). MSI-103 is thus found to realign in membranes at a much lower peptide concentration than

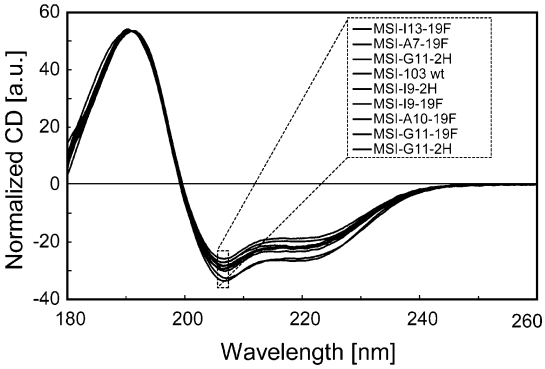

FIGURE 3: CD spectra in a 1:1 (v/v) TFE/buffer mixture of the MSI-103 analogues, normalized to the same value at 191 nm. All mutants show a very similar line shape as wild-type MSI-103, confirming a mostly α-helical conformation. The spectra are labeled in the inset according to their order at 208 nm.

PGLa. For the following NMR analysis of MSI-103, these OCD results are extremely useful, as they allow us to decide which concentration range to address with the more elaborate NMR measurements and how to interpret any differences in its behavior compared to that of PGLa.

Choice of Oriented or Nonoriented NMR Samples. Orientational constraints of membrane-bound peptides are most readily extracted using macroscopically oriented NMR samples on glass supports. Such samples are always measured with the bilayer normal parallel (0°) to the magnetic field. An additional experiment at a 90° sample inclination can then determine whether the peptide is motionally averaged by fast rotation around the membrane normal. All ^{19}F NMR experiments were performed on oriented samples over a wide range of peptide-to-lipid molar ratios (1:800 to 1:20). However, for the less sensitive ^{2}H NMR measurements, it is difficult to prepare oriented samples with a low peptide concentration, as a large amount of material would have to be accommodated on the solid supports in the NMR coil. Therefore, we decided to study only P:L values of 1:50 and 1:20 with oriented ^{2}H NMR samples, but to reach a P:L of 1:200, we used nonoriented multilamellar dispersions (MLV samples), which had been done previously for PGLa (*18*, *22*, *23*). As long as a peptide is motionally averaged by rotation about the membrane normal, the full information content can be extracted from MLV samples (as the Pake splitting then corresponds to half the splitting of an oriented sample measured at 0°). Any concentration ratios lower than 1:200 could not be addressed by ^{2}H NMR (only ^{19}F NMR), as the natural abundance background of the lipids becomes too dominant in such spectra. All oriented ^{2}H and ^{19}F NMR samples were examined by ^{31}P NMR to check the quality of alignment, and no conspicuous effect of the peptide of the phospholipids was noted.

^{19}F NMR Results. Five MSI-103 analogues were synthesized with L-4-CF_3-phenylglycine (CF_3-Phg) substituted for Ala7, Ile9, Ala10, Gly11, or Ile13 (see Table 1). Macroscopically oriented samples were prepared with P:L values of 1:800, 1:400, 1:200, 1:50, and 1:20 in DMPC. Representative ^{19}F NMR spectra are presented in Figure 5, and the dipolar splittings of the CF_3 groups are listed in Table 4. A comparison of the samples oriented with the bilayer normal parallel (0°) and perpendicular (90°) to the external magnetic field shows that the 90° splittings are always related to the 0° splittings by a factor of $-1/2$, except if P:L = 1:20. This

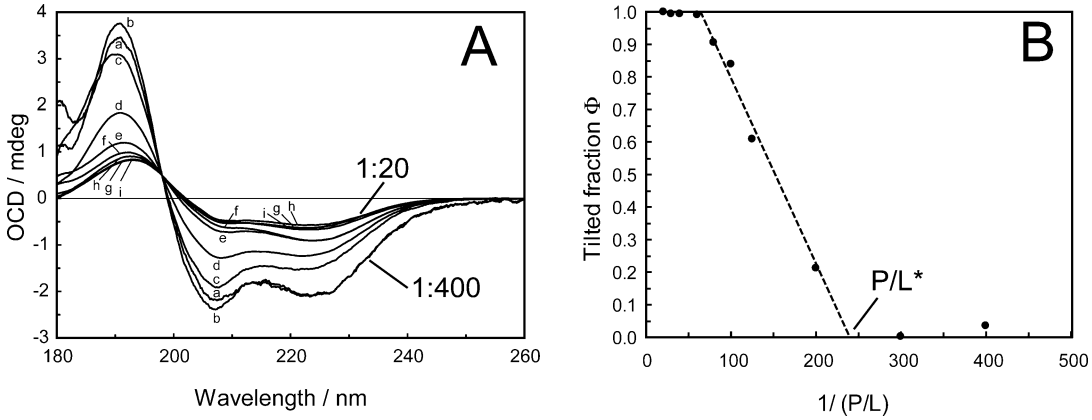

FIGURE 4: OCD results. (A) OCD spectra of MSI-103 in DMPC bilayers with different P:L ratios of (a) 1:400, (b) 1:300, (c) 1:200, (d), 1:125, (e) 1:100, (f) 1:80, (g) 1:40, (h) 1:30, and (i) 1:20. All curves are normalized to the same value at 198 nm. (B) Plot of the tilted fraction of peptides as a function of concentration. The linear part of the plot is fitted to a straight line (dashed) which gives the threshold concentration where the T-state starts to appear at a P:L* of 1:240.

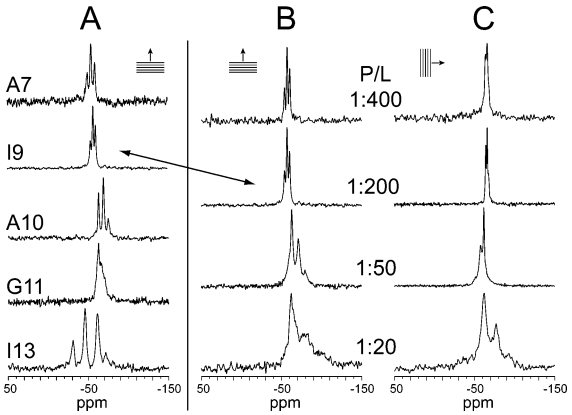

FIGURE 5: Representative ^{19}F NMR spectra of MSI-103 in oriented DMPC bilayers. (A) Analogues with CF_3-Phg labels at different positions, measured at a P:L of 1:200 with the bilayer normal parallel to B_0. (B) Spectra of MSI-I9-^{19}F at different P:L values, measured with the bilayer normal parallel to B_0. (C) Spectra of MSI-I9-^{19}F measured with the bilayer normal perpendicular to B_0 (the arrow indicates the same spectrum shown twice).

Table 4: ^{19}F NMR Dipolar Splittings (in kilohertz) of the CF_3-Phg-Labeled MSI-103 Analogues at Different Concentrations in Oriented DMPC Samples

	P:L (with sample orientation indicated as 0° or 90°)			
position labeled with CF_3-Phg	1:400 0°/90°	1:200 0°/90°	1:50 0°/90°	1:20 0°/90°
Ala7	+2.2/−1.0	+2.3/−1.1	−3.6/+1.7	+4.0/−1.9
Ile9	+1.5/−1.0	+1.5/−0.75	−3.9/+1.9	−8.0/−7.4
Ala10	−2.7/+1.3	−2.8/+1.4	−3.4[a]/+1.7	−6.1/−7.1
Gly11[b]	−5.1/+2.5	−1.8/+1[c]	−2.4/+1.2	−6.7/−7.0
Ile13	+6.7/−3.4	+7.1/−3.45	+6.7/−3.3	−7.8/−6.1

[a] Badly resolved, calculated from the shown splitting measured at 90°. [b] Data not shown for 1:800, but same splitting as for 1:400. [c] Splitting too small to observe, estimated value from 0°.

means that the peptide rotates fast around the bilayer normal at all concentration ratios up to 1:50. At a P:L of 1:20, on the other hand, the lines are much broader and most splittings are close to the value of −7.9 kHz, thus representing immobilized peptides with a powder distribution. Only for MSI-A7-^{19}F was a different splitting seen, and in this case, the peptide did rotate around the bilayer normal. We thus conclude that most of the CF_3-Phg-labeled peptides are aggregated at a P:L of 1:20 and no longer maintain a well-defined orientation in the membrane. At this very high concentration ratio, the NMR data therefore cannot be used to determine the structure of MSI-103, and only for the lower P:L range will the dipolar splittings be fitted in the following paragraphs to calculate the tilt and rotation of the helical peptide in the lipid bilayer. A first, visual inspection of the ^{19}F NMR data in Figure 5 suggests that MSI-103 must have a well-defined alignment at low concentrations up to 1:200 and that it reorients into a different alignment at 1:50, as suggested above by OCD.

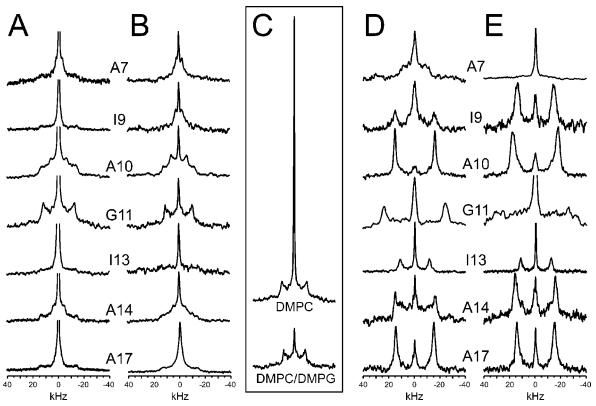

FIGURE 6: ^{2}H NMR spectra of MSI-103 labeled with Ala-d_3 at seven different positions (as numbered) and reconstituted in (A) DMPC at a P:L of 1:200. The central peaks are cut off. (B) DMPC/DMPG (3:1) at a P:L of 1:200, (D) DMPC at a P:L of 1:50, and (E) DMPC at a P:L of 1:20. The two samples at 1:200 (A and B) were prepared as multilamellar lipid dispersions and show Pake patterns, while the 1:50 and 1:20 samples (D and E) are macroscopically oriented and give defined splittings. The central panel (C) shows a comparison of the full spectra of MSI-G11-^{2}H in DMPC and in DMPC/DMPG MLV samples at a P:L of 1:200, to illustrate the enhanced binding of the cationic peptide to negatively charged lipids.

^{2}H NMR Results. The ^{2}H NMR spectra of seven MSI-103 analogues labeled with Ala-d_3 at positions Ala7, Ile9, Ala10, Gly11, Ile13, Ala14, and Ala17 are shown in Figure 6, for three different peptide-to-lipid ratios (1:200, 1:50, and 1:20). At a low concentration ratio of 1:200 in DMPC (Figure 6A), the spectra of the nonoriented MLV samples reveal a different Pake splitting for each of the analogues. However, these signals are always overlapped by another component with a constant splitting of ∼26 kHz, which is attributed to natural abundance deuterons in the lipids, as demonstrated

Table 5: ^{2}H NMR Quadrupole Splittings (in kilohertz) of the Ala-d_3-Labeled MSI-103 Analogues at Different Concentrations in Various Lipid Samples

position labeled with Ala-d_3	MSI-103/DMPC (1:200) MLV samples	MSI-103/DMPC/DMPG (1:150:50) MLV samples	MSI-103/DMPC (1:50) oriented samples	MSI-103/DMPC (1:20) oriented samples
Ala7	8.6[a]/4.3[b]	8.8[a]/4.4[b]	17.0[c]	2.0[c]
Ile9	12.0[a]/6.0[b]	9.4[a]/4.7[b]	30.4[c]	28.5[c]
Ala10	24.1[a]/12.0[b]	24.2[a]/12.1[b]	31.2[c]	35.2[c]
Gly11	48.2[a]/24.1[b]	42.0[a]/21.0[b]	47.5[c]	Ca 60[c,d]
Ile13	4.0[a]/2.0[b]	4.2[a]/2.1[b]	22.8[c]	23.9[c]
Ala14	14.8[a]/7.4[b]	15.4[a]/7.7[b]	31.0[c]	31.5[c]
Ala17	13.4[a]/6.7[b]	16.2[a]/8.1[b]	29.7[c]	29.5[c]

[a] Pake splittings from nonoriented MLV samples multiplied by two, corresponding to the 0° edge, for comparison with the oriented samples. [b] Pake splittings measured from nonoriented MLV samples at the 90° peaks (Figure 6). [c] Splittings of the oriented samples aligned at 0° (spectra in Figure 6). [d] Splitting not well-defined.

previously by ^{2}H NMR of pure DMPC (*22*). Even worse, a third, large isotropic component is seen in these ^{2}H NMR spectra, which is likely to contain a small amount of residual deuterium from HDO in the water. The majority of this central component, however, is attributed to free peptide molecules tumbling rapidly in solution, as reported previously for PGLa in MLV samples containing a slight excess of water (*22*). It was argued that the cationic peptides can escape from the zwitterionic DMPC vesicles, and MSI-103 is even more charged and indeed highly water soluble. The spectra show that the free peptide molecules are not in fast exchange with the membrane-bound population giving rise to the anisotropic splittings; however, in some cases, these splittings are so small that they cannot be resolved in the presence of the dominant isotropic peak.

The best way to avoid the isotropic component is to use macroscopically oriented samples, as they are prepared at 96% humidity and do not contain any excess water. However, as explained above, it is hard to observe ^{2}H NMR signals from such samples at low peptide concentrations. Therefore, we decided to prepare instead another series of MLV samples consisting of MSI-103, DMPC, and DMPG at a 1:150:50 ratio. The presence of the negatively charged dimyristoylphosphatidylglycerol (DMPG) keeps the peptide electrostatically attracted to the membrane and significantly reduces the isotropic spectral component, as seen in Figure 6B. Note that the isotropic peaks in Figure 6A are cut off in the display, but in Figure 6C, the full height of the spectra is compared for MSI-G11-^{2}H in DMPC and in DMPC/DMPG bilayers, illustrating the larger isotropic peak using uncharged membranes. The spectra in Figure 6B demonstrate that the quadrupolar splittings are essentially the same for the MSI-103 analogues in DMPC/DMPG bilayers (3:1) and in pure DMPC (see also Table 5). We thus conclude that the alignment of the membrane-bound peptide does not change in the presence of DMPG, but this set of ^{2}H NMR data can be analyzed much more readily in MLV samples.

At the higher peptide concentrations of 1:50 (Figure 6D) and 1:20 (Figure 6E), a single quadrupole splitting is seen for each MSI-103 analogue in the oriented DMPC samples (Table 5). These data show that the peptide has a unique and well-defined orientation in the membrane at these higher concentrations, which differs from its alignment at a P:L of 1:200 (Figure 6B). We thus conclude that MSI-103 undergoes a concentration-dependent realignment in the DMPC bilayer, as suggested above by ^{19}F NMR and OCD.

Table 6: Best-Fit Values for Different Helical Structures Using ^{2}H NMR Data

data set	model	tilt angle τ (deg)	rotation angle ρ (deg)	S_{mol}	rmsd (kHz)
DMPC, 1:200	α-helix	111	122	0.65	1.6
	π-helix	72	140	1.00	4.7
	3_{10}-helix	52	82	1.00	11.0
DMPC, 1:50	α-helix	128	105	0.83	3.1
	π-helix	43	151	0.72	9.1
	3_{10}-helix	96	108	0.84	7.7

Analysis of the Peptide Conformation. To describe the alignment and dynamics of a folded peptide in terms of τ, ρ, and S_{mol} (see Materials and Methods), its conformation in the bilayer has to be known. MSI-103 was shown by CD to form a helical structure in a membraneous environment (Figures 3 and 4). In our previous analysis of PGLa, we had attempted to fit the ^{19}F NMR data to several different helical conformations and found that a π-helix or a 3_{10}-helix model did not support the data (*13*). Only the α-helical model based on polyalanine gave good fits; hence, this model was also used for all subsequent ^{2}H NMR data analyses of PGLa (*18*, *22*, *23*). Here, for MSI-103 we also tried the three types of helices for fitting the ^{2}H NMR data at 1:200 and 1:50 in DMPC. Of the seven Ala-d_3 labels used, four of them are entirely unperturbing; hence, the risk of a structural perturbation or a misfit is low (see the discussion of the ^{2}H NMR data below). The resulting quality of the fits is summarized in Table 6 and can be judged in terms of the root-mean-square deviation (rmsd). We found that an α-helical model gives much better fits at both concentrations compared to the other helical models. Especially the 3_{10}-helix gives unacceptably high rmsd values, and at 1:200, both 3_{10}- and π-helix would require an order parameter S_{mol} of 1.0, which is not reasonable for unaggregated peptides in fluid bilayers. In dry powder samples of Ala-d_3-labeled peptides, a splitting of ca. 37 kHz is found (data not shown), meaning that already in a dry powder there is some peptide motion which leads to an averaging of splittings, corresponding to an S_{mol} of 0.88. In a highly mobile lipid bilayer, it is unlikely that there would be less motion of peptides than in a dry powder. We have previously found S_{mol} to be 0.6−0.7 at a low peptide concentration for PGLa (*13*, *17*, *18*, *22*), which fits nicely with the value found here for an α-helical conformation of MSI-103. Considering the primary sequence of MSI-103, it is also clear that the α-helical conformation represents a pronounced amphiphilic profile with all charged lysine residues on one face of the peptide (see Figure 1). This is

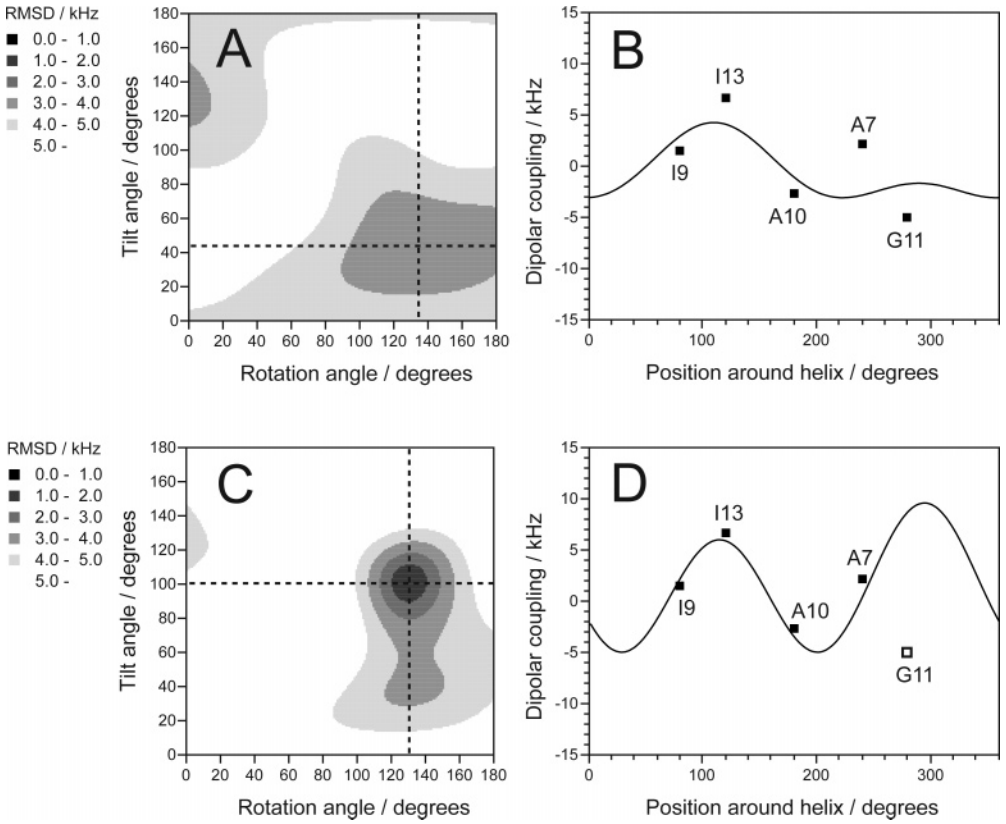

FIGURE 7: (A) Error plot for MSI-103 in DMPC bilayers at 1:400, using the ^{19}F NMR data from all five labeled positions. (B) Corresponding quadrupolar wave plot, with the best-fit curve to all five data points identified by residue numbers. (C) Error plot calculated from only the four data points of the biologically active analogues with CF_3-Phg at Ala7, Ile9, Ala10, and Ile13. (D) Corresponding quadrupolar wave plot, in which the data point of Gly11 (□) is not used for fitting.

Table 7: Best-Fit Orientation Parameters for MSI-103 in DMPC Lipid Bilayers from ^{19}F NMR Data

P:L	labels used	tilt angle τ (deg)	rotation angle ρ (deg)	S_{mol}	rmsd (kHz)
1:400	CF_3 at A7, I9, A10, G11, I13	43	135	0.39	3.1
1:200	CF_3 at A7, I9, A10, G11, I13	60	137	0.32	2.6
1:50	CF_3 at A7, I9, A10, G11, I13	32	115	0.52	3.1
1:400	**CF_3 at A7, I9, A10, I13**	**101**	**130**	**0.63**	**1.1**
1:200	CF_3 at A7, I9, A10, I13	102	129	0.69	1.2
1:50	CF_3 at A7, I9, A10, I13	109	113	1.00	0.7

not the case for the π-helix or 3_{10}-helix conformations, which would not be energetically favorable when bound to a membrane. On the basis of this analysis and in line with previous PGLa studies (*17*, *18*, *22*, *23*), we therefore used an ideal α-helix as a model structure for MSI-103 at all concentrations to fit the ^{2}H and ^{19}F NMR data.

Helix Alignment from ^{19}F NMR Data. At very low peptide concentrations, the amphiphilic α-helical MSI-103 is expected to bind as a monomer to the membrane surface with an almost flat orientation. This would correspond to a tilt angle τ of ~90°, and an azimuthal rotation ρ that positions the charged lysine side chains up toward the water, in a fashion similar to that of other amphipathic peptides like PGLa (*17*, *18*, *22*). However, the best fit for a P:L of 1:400 using our five ^{19}F NMR data points seems to produce a tilt angle of ~43° and a large rmsd (Table 7). Figure 7A shows the corresponding two-dimensional error plot for MSI-103 in DMPC at a P:L of 1:400, based on all five CF_3-Phg labels in the analysis. Here, the error (in kilohertz) is depicted by a grayscale for all combinations of τ and ρ. If we had also wanted to display the dependence on the order parameter, this would require a three-dimensional error plot; hence, we show only the τ/ρ map obtained for the best-fit order parameter value (S_{mol}) of 0.39. This is very small compared to the values previously found for PGLa, which were usually around 0.6−0.7. It is also conspicuous that no minimum with a rmsd below 2 kHz exists. The corresponding dipolar wave plot for the best-fit values of τ, ρ, and S is shown in Figure 7B and represents the nominal peptide structure ($\tau = 43°$, $\rho = 137°$, and $S_{mol} = 0.39$). In this plot, the hypothetical dipole splittings are calculated for each position around the helical wheel and displayed on a curve from 0° to 360°. The curve clearly does not fit well to the five data points.

Since the peptide mutant in which Gly11 had been substituted with CF_3-Phg had exhibited a much lower antimicrobial activity than the wild type and all the other MSI-103 analogues (see Table 2), we decided to exclude MSI-G11-^{19}F and fitted the ^{19}F NMR data of the remaining four labels only. The resulting error plot is shown in Figure 7C and the dipolar wave in Figure 7D. In this case, a much better fit was found, with a rmsd of 1.1 kHz. Now, the tilt angle (τ) of 101° corresponds to the expected S-state

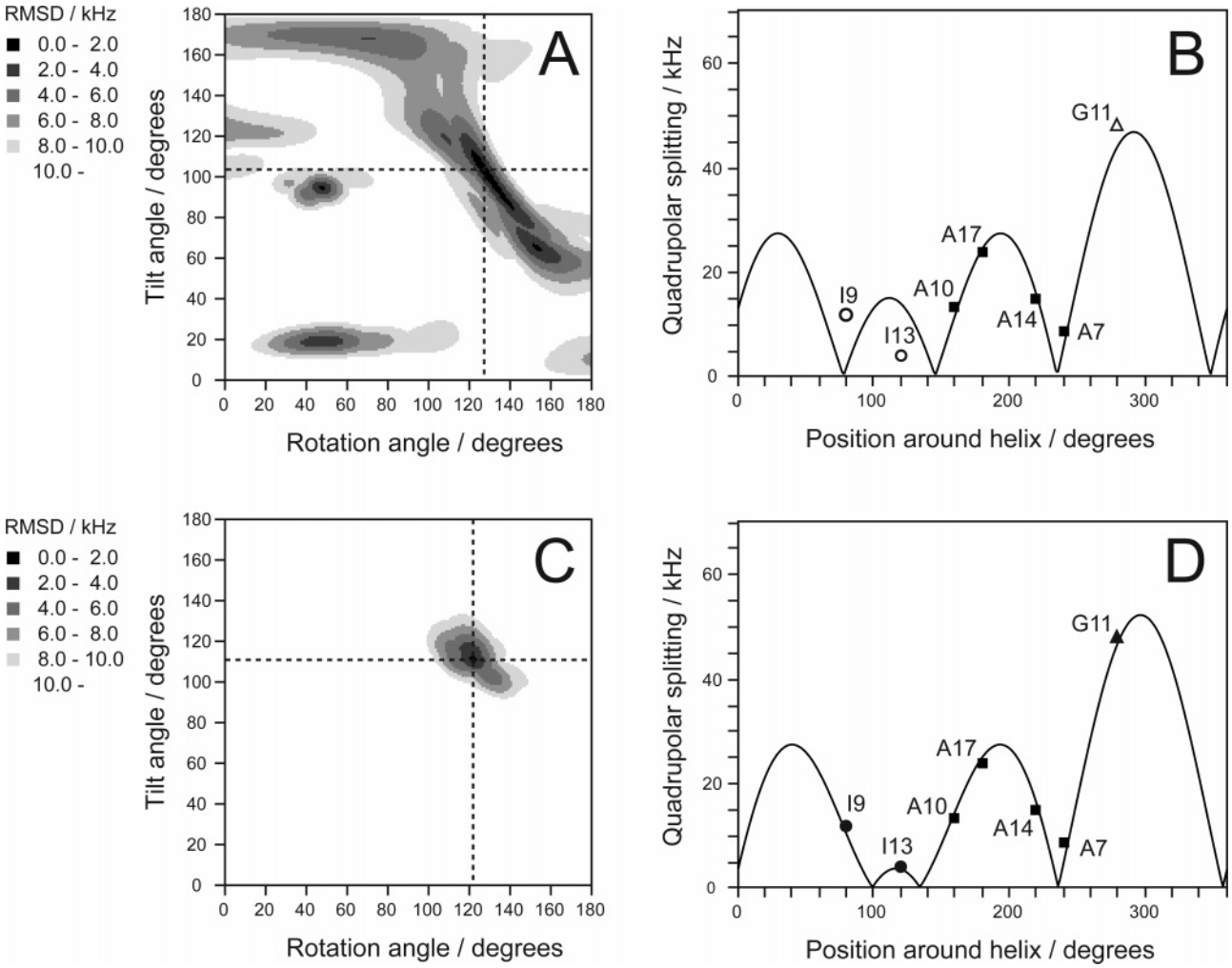

FIGURE 8: (A) Error plot for MSI-103 in DMPC bilayers at 1:200, using only the ^{2}H NMR data from the four nonperturbing Ala-d_3 substitutions at positions Ala6, Ala8, Ala10, and Ala14. (B) Corresponding quadrupolar wave plot, fitted to the four native Ala positions (■). The experimental splittings from two Ile positions (○) and one Gly (△) are also shown but not used in the fit. (C) Error plot calculated from all seven labeled Ala-d_3 positions, showing a unique minimum as the best-fit solution. (D) Corresponding quadrupolar wave plot with the curve calculated from all seven data points.

orientation of the peptide on the membrane surface. The fact that the numerical value of the tilt angle is higher than 90° means that the amidated C-terminus is inserted slightly deeper into the membrane than the charged N-terminus. The observed rotation angle ρ of 130° perfectly positions all charged lysine residues on the hydrophilic face of the peptide toward the aqueous phase. This alignment of MSI-103 fits well with the orientation found previously for PGLa (also using four ^{19}F labels) (*13*). If the functionally inactive peptide analogue is excluded, the four data points are readily fitted by three parameters, and the resulting structure makes sense. However, in view of the few data points, it must be noted that the best-fit values are rather sensitive to errors in the data, and the structure should be taken as approximate, with an error of ±10° in τ and ρ.

For a P:L of 1:200, the ^{19}F NMR analysis gave a result similar to that at 1:400. Also at this concentration, a fit using all five labels gave an unexpectedly small tilt angle and order parameter, and a very large rmsd, but if the mutant MSI-G11-^{19}F is excluded, the analysis using the other four data points gave the same tilt and rotation angles as at 1:400, with a similar rmsd and almost the same order parameter (see Table 7). As seen in Table 4, this label at Gly11 is also the only one whose splitting changes significantly on going from 1:400 to 1:200. We thus conclude that at low concentration ratios (1:400 and 1:200) MSI-103 has the expected S-state orientation in DMPC. Only the splitting of the mutated peptide with CF_3-Phg at position Gly11 is not consistent with the data set. This observation is not too surprising, since among all mutations this one represents the most dramatic change in volume. The strongly increased hydrophobicity of CF_3-Phg at the otherwise moderately hydrophilic position 11 might force the peptide to rotate so that it can be immersed deeper into the hydrocarbon region of the membrane (see the helical wheel in Figure 1). An alternative explanation could be attributed to an increased propensity for peptide−peptide interactions to occur on this face, which could introduce a population of dimers or aggregates. To investigate whether MSI-G11-^{19}F may have undergone premature oligomerization at 1:400, an additional sample with a P:L of 1:800 was prepared for this label, but it gave the same splitting as 1:400 (data not shown). It thus seems that this mutant has an intrinsically different orientation even from the monomeric wild-type MSI-103. Overall, we conclude that MSI-103 and its biologically active CF_3-Phg-labeled analogues have an orientation very similar to that of PGLa in a DMPC bilayer (*13*) at low peptide concentrations.

Table 8: Best-Fit Orientation Parameters for MSI-103 in Lipid Bilayers from ^{2}H NMR Data

P:L	labels used	tilt angle τ (deg)	rotation angle ρ (deg)	S_{mol}	rmsd (kHz)
		DMPC			
1:200	CD_3 at A7, A10, A14, A17	63	148	0.62	1.8
1:50	CD_3 at A7, A10, A14, A17	135	90	0.81	0.8
1:20	CD_3 at A7, A10, A14, A17	123	109	0.98	2.1
1:200	**CD_3 at A7, I9, A10, G11, I13, A14, A17**	**111**	**122**	**0.65**	**1.6**
1:50	**CD_3 at A7, I9, A10, G11, I13, A14, A17**	**128**	**105**	**0.83**	**3.1**
1:20	**CD_3 at A7, I9, A10, G11,[a] I13, A14, A17**	**125**	**109**	**0.92**	**3.5**
		DMPC/DMPG			
1:200	CD_3 at A7, A10, A14, A17	61	160	0.59	0.2
1:200	CD_3 at A7, I9, A10, G11, I13, A14, A17	111	122	0.60	1.7

[a] Value too uncertain to be used in the fit, but consistent with the remaining best-fit curve.

At a P:L of 1:50, the ^{19}F NMR spectra show that MSI-103 is still rotationally averaged around the bilayer normal, but the dipolar splittings are not the same as at lower peptide concentrations, indicating a change in the orientation of the helix. When all of the five data points were used to calculate the orientation, a very different tilt (32°) was found and the rmsd was extremely high, 3.1 kHz (Table 7). Excluding the perturbing CF_3-Phg label at Gly11 again gave a better fit, with a tilt angle (τ) of 109° and an azimuthal rotation angle (ρ) of 113°, and a reasonable rmsd, but the S_{mol} value was unrealistically high, 1.0, which would correspond to a totally immobilized peptide. When S_{mol} was fixed to a more normal value of 0.7, a best-fit solution was found with a τ of 107°, a ρ of 112°, and a rmsd of 1.7 kHz, which is almost the same alignment but again with a large error. Therefore, we conclude that the conformation of the CF_3-Phg-labeled MSI-103 analogues appears to be distorted from an ideal α-helix at high concentrations, possibly due to suboptimal contacts at a dimerization interface (see below).

The analysis of ^{19}F NMR data given above was performed using α-helical model B (see the description in Materials and Methods). Similar results were obtained using helix model A (which was used for the ^{2}H NMR analysis) but in general with higher rmsd, and therefore, we here show the results using model B which gave better fits. The results using model A are presented as Supporting Information.

Helix Alignment from ^{2}H NMR Data. The substitution of a proton with ^{2}H does not perturb the chemical properties of a molecule; hence, a substitution of a native Ala residue (at position 7, 10, 14, or 17) with Ala-d_3 will not affect the behavior of wild-type MSI-103. However, when any other amino acid is replaced with Ala-d_3, the mutation might change the properties of the peptide. To analyze MSI-103 in an entirely unperturbed conformation, we thus started off using only the ^{2}H NMR data from the four native Ala positions. At a P:L of 1:200, no clear-cut result was obtained, as the two-dimensional error plot in Figure 8A contains several minima with a rmsd below 2.0 kHz. Figure 8B shows the quadrupolar wave corresponding to the lowest rmsd, but this result is not yet trustworthy, since the signs of the quadrupole splittings are not known. For such ^{2}H NMR analysis, it is clear that more than four data points (i.e., absolute splittings) are needed to determine the orientation of a peptide uniquely, in contrast to the use of four signed splittings in the ^{19}F NMR analysis described above. When three additional quadrupole splittings from the Ala-d_3 labels at positions Ile9, Gly11, and Ala13 are included in the ^{2}H NMR analysis, a unique rmsd minimum is obtained (Figure 8C). All seven data points fit well on the quadrupolar wave, as illustrated in Figure 8D, suggesting that the labeled stretch is consistent with an unperturbed α-helical conformation over its full length. When the rmsd values are being compared between ^{19}F and ^{2}H NMR data, it should be remembered that ^{2}H splittings are 5.3 times larger so that a ^{19}F rmsd of 1 kHz corresponds to a ^{2}H rmsd of 5.3 kHz. The relative error is thus smaller for the fit from ^{2}H data than that found above for ^{19}F data. The rmsd minimum corresponds to a helix tilt angle (τ) of 111°, a rotation angle (ρ) of 122°, and an order parameter (S_{mol}) of 0.65 in DMPC, and in DMPC/DMPG (3:1) bilayers, very similar results are obtained (Table 8). This structure describes the alignment of the MSI-103 helix in DMPC and in DMPC/DMPG bilayers such that its C-terminus is inclined ∼20° away from the membrane surface toward the bilayer interior. The rotation angle of 122° shows that the charged lysine residues are directed toward the aqueous phase. Since all data points fit well together, we conclude that the structure and orientation of MSI-103 at 1:200 are not influenced by a substitution of a small glycine residue or a bulky isoleucine side chain with an Ala-d_3 label.

At higher peptide concentration ratios of 1:50 and 1:20, the use of only four nonperturbing Ala-d_3 labels was also insufficient to obtain a reliable structure; hence, all seven labels had to be used in the analysis. This is demonstrated in panels A and C of Figure 9, showing the error plots at a P:L of 1:50 using only four labels and all seven labels, respectively. The corresponding quadrupolar curves are illustrated in panels B and D of Figure 9. The analysis was also carried out for a peptide-to-lipid ratio of 1:20, as seen in panels E and F of Figure 9. Both peptide-to-lipid ratios give practically the same result: at 1:50, $\tau = 128°$, $\rho = 105°$, and $S_{mol} = 0.83$, and at 1:20, $\tau = 125°$, $\rho = 109°$, and $S_{mol} = 0.92$ (Table 7). This alignment of MSI-103 is very close to the picture found previously for PGLa in DMPC and DMPC/DMPG bilayers at high concentrations, which had been named the tilted T-state (*17*, *18*, *22*). In both peptides, at high concentrations the helix tilt angle is ∼25° larger than at low concentrations (from ^{19}F NMR at 1:400), while the azimuthal rotation angle is somewhat smaller. The order parameter is somewhat larger than at low concentrations, indicating a lower degree of wobbling with an increase in concentration. The ^{2}H NMR spectra of the oriented samples rotated to 90° (data not shown) demonstrate that at 1:50 and 1:20 the peptide has stopped rotating around the bilayer normal. This finding indicates that at high peptide concentrations the helices are laterally immobilized in the membrane,

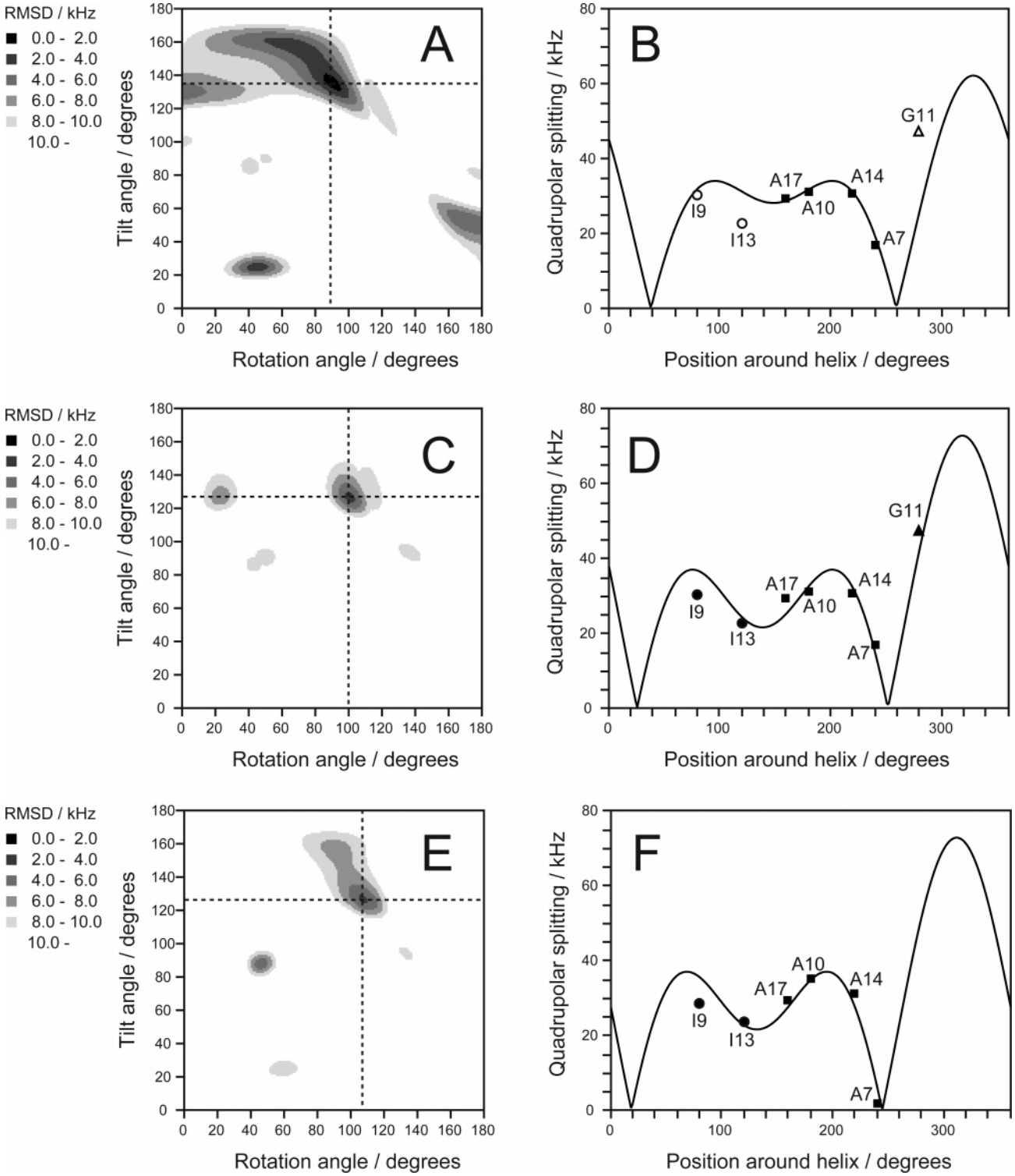

FIGURE 9: (A) Error plot for MSI-103 in DMPC bilayers at 1:50, using only the ^{2}H NMR data from the four nonperturbing Ala-d_3 substitutions. (B) Corresponding quadrupolar wave plot, fitted only to the four native Ala positions (■). The experimental splittings from two Ile positions (○) and one Gly (△) are also shown but not used in the fit. (C) Error plot calculated from all seven labeled Ala-d_3 positions. (D) Corresponding quadrupolar wave plot from all seven data points. (E) Error plot for MSI-103/DMPC bilayers at 1:20, calculated from six labeled Ala-d_3 positions (Gly11 not used). (F) Corresponding quadrupolar wave plot at 1:20 calculated from six data points.

while still maintaining a specific tilt angle and azimuthal rotation angle.

DISCUSSION

In this study, we have used solid-state ^{19}F and ^{2}H NMR on selectively CF_3-Phg- and Ala-d_3-labeled MSI-103 analogues, to determine the orientation of this antimicrobial peptide in DMPC bilayers at different concentrations. First, we will compare the MSI-103 results at low and high peptide concentrations. Then, the structures will be compared with previous results for the related peptide PGLa. Finally, the differences between MSI-103 and PGLa in terms of their reorientation and dynamic behavior will be discussed in light of their antimicrobial and hemolytic activities.

Surface-Bound S-State of MSI-103 at Low Concentrations. The range of low peptide-to-lipid ratios is best addressed by highly sensitive ^{19}F NMR measurements of CF_3-Phg labels, which provide sufficient signal intensity even at concentrations as low as 1:800. Up to a P:L of 1:200, the structure analysis of MSI-103 gave a consistent picture of the helical peptide being aligned in the surface-bound S-state, with a tilt angle (τ) of ~101° (see Table 7 and Figure 7C,D). The azimuthal rotation angle of ~130° is fully consistent with the amphiphilic profile of MSI-103, and the value of S_{mol} of ~0.65 suggests a monomeric state. As seen from the samples measured at a 90° alignment, the peptide is free to rotate about the membrane normal on the millisecond time scale of the NMR experiment.

With an increase in the peptide concentration to 1:50, the ^{19}F NMR splittings of all labels were found to change compared to those in the low-concentration regime, indicating a change in the orientation of the helix (see Figure 5). MSI-103 still rotates around the bilayer normal, according to the 90° sample alignment. However, the fit to the four relevant ^{19}F NMR data points is not convincing, giving either a τ of 109° and a ρ of 113° with an alarming S_{mol} value of 1, or when a reasonable S_{mol} is fixed, then the rmsd becomes very high (see Table 7). Besides the position of Gly11 that becomes perturbed by CF_3-Phg substitution, it seems that at high concentrations some other positions of MSI-103 are also sensitive to mutations, due to changes in hydrophobicity or dimerization contacts. The poor fit suggests that the ^{19}F NMR data should not be considered to represent an accurate orientation of MSI-103 at a P:L of 1:50. According to the OCD analysis, the wild-type peptide exists as a mixture of S- and T-states between 1:60 and 1:240 (Figure 4). It is conceivable that the individual CF_3-Phg-labeled analogues may have slightly different equilibrium thresholds and that some of the peptides may not have reached a pure T-state at 1:50, so the fit would not work. At 1:20, all peptide analogues should clearly be in the T-state, but unfortunately at that concentration, the ^{19}F NMR spectra (unlike ^{2}H NMR) showed peptide aggregation and no fit was possible.

Tilted T-State of MSI-103 at High Concentrations. Given the difficulties of the ^{19}F NMR data at high concentrations, this range is better examined by ^{2}H NMR. Here, we obtain two self-consistent sets of data at P:L values of 1:50 and 1:20, both of which yield essentially the same picture of a tilted peptide in the T-state (see Figure 9). The helix tilt angle is found to have increased to around 125°; ρ has decreased slightly to 105°, and the order parameter S_{mol} approaches 0.8 at 1:50 and 0.9 at 1:20 (see Table 8). These parameters are consistent with the hypothesis that - just like PGLa (*18*, *22*), the peptides have assembled into antiparallel dimers and the changes in tilt and azimuthal angles reflect the preferred packing of helices in this stable and distinct state.

Realignment of MSI-103 from the S-state to the T-state occurs over a broad concentration range from 1:240 to 1:60, according to the OCD analysis, with a threshold around 1:240. It is more difficult to extract such a threshold quantitatively from the NMR data. Both analyses by ^{2}H and ^{19}F NMR clearly indicate that the change in tilt angle occurs between 1:200 and 1:50. However, according to ^{19}F NMR, the alignment of MSI-103 at 1:200 still corresponds completely to the S-state, whereas ^{2}H NMR suggests an alignment that is halfway between the S- and T-states [$\tau = 111°$ and $\rho = 122°$ (see Table 8 and Figure 8)]. A similar intermediate situation had been previously encountered for PGLa and was interpreted as a 55:45 mixture of S- and T-states in fast exchange, leading to an averaging of the quadrupolar splittings (*22*). Since the relative error of the ^{2}H NMR fit with seven Ala-d_3 labels is smaller than for the ^{19}F NMR data with four CF_3-Phg labels, we trust that the intermediate alignment of MSI-103 at 1:200 in DMPC represents a more accurate and reliable result. Figure 10 summarizes the course of realignment of MSI-103, using the data we consider most reliable (highlighted in boldface text in Tables 7 and 8). Overall, an intrinsic error of ±3° in τ and ρ from ^{2}H NMR and approximately twice as much for ^{19}F NMR should be taken into account, given the assumption that MSI-103 has a perfectly helical conformation.

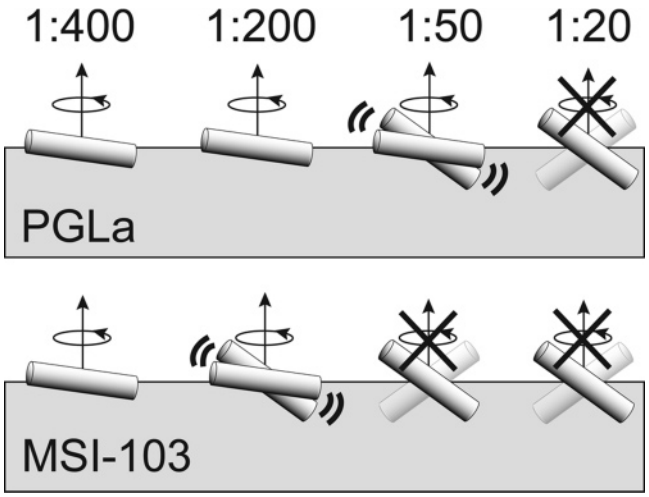

FIGURE 10: Comparison of the structural and dynamic behavior of MSI-103 and PGLa as a function of the peptide-to-lipid ratio in a DMPC bilayer. The realignment from a surface-bound S-state to a tilted T-state occurs at a lower threshold concentration for MSI-103 than for PGLa. Fast exchange between S- and T-states is illustrated by overlapping peptides with dynamic wings. The formation of homodimers in the T-state is represented by the presence of a second semitransparent peptide. Fast motional averaging of a peptide about the membrane normal is indicated by a circular arrow, which is crossed out where this rotation has ceased and the peptides are laterally immobilized. The PGLa ^{2}H NMR data are taken from ref *22* [1:200 (MLV), 1:50 (MLV), 1:20 (oriented), and 1:400 (proposed S-state)]. The MSI-103 results are from this study [1:400 (oriented) from ^{19}F NMR, model B; 1:200 (MLV) from ^{2}H NMR; 1:50 (oriented) from ^{2}H NMR; and 1:20 (oriented) from ^{2}H NMR].

Another subtle difference between the ^{2}H and ^{19}F NMR data concerns the dynamic behavior of MSI-103 in the T-state. By ^{2}H NMR, the peptides were found to have stopped rotating around the bilayer normal at a P:L of ≥1:50, but they still maintained their alignment with respect to the membrane surface [using both MLV and oriented samples (data not shown)]. The ^{19}F NMR spectra suggested a more extreme change in dynamics, namely that the peptides were still averaged about the membrane normal at 1:50, while at 1:20 they not only stopped to rotate but also had lost their alignment in the membrane. Again, these differences might be attributed to slight differences in the equilibrium thresholds of the individual ^{19}F-labeled peptides on which the analysis was based. The qualitative agreement between the ^{2}H and ^{19}F NMR data is nevertheless remarkable, despite these subtle differences in the absolute concentration range over which the realignment or change in dynamics occurs.

Table 9: Change in Hydrophobicity and Hemolytic Activity of Mutated MSI-103 Compared to the Original Peptide

	A7-^{19}F	I9-^{19}F	A10-^{19}F	G11-^{19}F	I13-^{19}F	I9-^{2}H	G11-^{2}H	I13-^{2}H
hydrophobicity	↑	↓	↑	↑	↓	↓	↑	↓
hemolysis	↑	↓	↑	↑	↓	↓	↑	↓

Comparison of MSI-103 with PGLa. MSI-103 is a product of rational drug design, whose sequence was derived from PGLa, a peptide found in the skin of the frog *X. laevis* (*3*, *25*). It is therefore of interest to compare these results with our earlier NMR studies of the parent peptide. ^{19}F NMR analysis of CF_3-Phg-labeled PGLa showed that this helical peptide lies flat on the membrane surface in an S-state at 1:200, and it assumes a tilted T-state at 1:50 (*13*, *17*). ^{2}H NMR using eight Ala-d_3 labels gave a more accurate and comprehensive picture, showing that the orientational equilibrium is influenced not only by peptide concentration but also by sample hydration and lipid composition (*18*, *22*). In fully hydrated MLV samples with 1:200 PGLa in DMPC, a tilt angle of 98° and an azimuthal rotation of 115° were found to describe the S-state appropriately. Oriented samples at 1:50, on the other hand, yielded a characteristic and stable T-state with a τ of 126° and a ρ of 110° (*18*). In oriented samples at 1:100 and 1:20, very similar τ and ρ values were found, differing by only a few degrees from the 1:50 samples (*22*). The same distinct S- and T-states were also observed for PGLa in mixed DMPC/DMPG (3:1) bilayers. Given the known tendency of related antimicrobial peptides to dimerize, the S- and T-states were interpreted as monomeric and dimeric forms of PGLa, respectively (*22*). More recently, a third orientational state was discovered for PGLa in the presence of an equimolar amount of magainin 2, suggesting that heterodimers can be formed. The nearly upright orientation of the helices in an inserted I-state enables the peptides to span the membrane (*23*). Assembly of several such dimers as a stable transmembrane pore would explain the known synergistic effect, i.e., the improved antimicrobial action of PGLa in combination with magainin 2 against bacteria.

In MSI-103, a peptide with an amino acid composition and amphipathic profile similar to those of PGLa, we now also find an S-state and a T-state. Figure 10 gives an overview of the concentration-dependent realignment of the two related peptides in DMPC bilayers as observed by ^{2}H NMR. The properties in the T-state at 1:20 are strikingly similar; hence, we propose that both peptides form homodimers in a similar way, with the same preferred orientation and possibly the same dimerization interface. However, the threshold for dimerization is significantly lower for MSI-103 than for PGLa. With an increase in concentration, MSI-103 already starts to tilt at 1:200, while PGLa reaches a fast exchange between S- and T-states only at 1:50 in DMPC (*22*). According to this interpretation, a pure S-state for MSI-103 can be observed only at concentrations well below 1:200. Unfortunately, ^{2}H NMR is too insensitive for such oriented samples, and MLV samples are unsuitable due to the high solubility of MSI-103 in water and the disturbing background signals from water and lipids. ^{19}F NMR, on the other hand, has not provided us with sufficient accuracy to discriminate a pure S-state from a fast exchange between S- and T-states; hence, Figure 10 is meant to illustrate at 1:400 a "very low" concentration. Overall, the different dimerization thresholds for MSI-103 and PGLa are supported by several other observations besides the accurate ^{2}H NMR tilt angle analysis. The fact that MSI-103 in the T-state at 1:50 does not rotate around the bilayer normal, which is the case for PGLa at this concentration, indicates that MSI-103 has a stronger propensity to form extended assemblies. For PGLa, such assemblies with no rotation around the bilayer normal were found only at 1:20 (*22*). From OCD, the threshold concentration for realignment of MSI-103 in DMPC bilayers is found to be 1:240, while for PGLa, it has been reported to be ~1:80. This independent result also indicates that MSI-103 has a stronger propensity to dimerize than PGLa.

An in-depth NMR structure analysis of PGLa suggested that the mutual stabilization of two tilted peptides within a dimer is the most adequate explanation of the otherwise surprising observation of an oblique helix tilt angle (*22*). Besides these postulated homodimers, PGLa has also been shown by ^{2}H NMR to form 1:1 heterodimers with the related peptide magainin 2 from the same organism, for which a pronounced synergistic activity has been described (*23*). Many other helical antimicrobial peptides have a tendency to dimerize, as demonstrated in solution as well as in the solid state (*19*, *49*−*51*). Compared to these natural sequences, however, it is remarkable that the synthetic MSI-103 peptide can also assemble into dimers, since its KIAGKIA repeat sequence was artificially designed and empirically selected to be the most potent drug candidate. Unlike PGLa, MSI-103 cannot have evolved a specific dimerization interface for optimal function as a homodimer. Nevertheless, it appears that this successful drug candidate bears the same dimerization propensity in its regular amphiphilic structure, and this appears to contribute to its biological function.

The dimerization of MSI-103 in the solid state has been previously demonstrated by REDOR measurements on selectively ^{13}C- and ^{19}F-labeled peptides (named K3 in that publication) (*21*). Toke et al. collected several distance constraints in dipalmitoylphosphatidylcholine/dipalmitoylphosphatidylglycerol (1:1) bilayers, from which the putative dimerization interface could be inferred. According to the REDOR data, MSI-103 was suggested to form a parallel dimer via its Ala-rich surface, and such dimers were found to coexist with monomeric peptides. Such monomer−dimer equilibrium is in good agreement with the concentration-dependent realignment of MSI-103 from a monomeric S-state to a dimeric T-state observed here by OCD and ^{2}H and ^{19}F NMR. On the other hand, on the basis of symmetry arguments, our NMR data support the formation of an antiparallel head-to-tail dimer better than any parallel structure. The fact that only a single set of NMR splittings is seen for any one label suggests that both parts of the dimer must have the same orientation with respect to the membrane plane. Among all putative dimeric geometries (side-by-side, back-to-back), the only reasonable solution of two helices consistent with these arguments is an antiparallel arrangement, assuming that both peptides reside on the same face of the lipid bilayer.

The two dimeric models discussed here differ in yet another aspect, namely, the helix tilt angle and its membrane immersion. It was suggested by Toke et al. that both the monomeric and dimeric units are assembled into a toroidal wormhole, forming a transmembrane pore in the lipid bilayer (*21*). However, the orientation of the peptide helices was not accessible from these REDOR data; hence, no reliable conclusion could be drawn about the peptide alignment in that study. Here, from our orientational NMR constraints, it was possible for the first time to determine the tilt angle of MSI-103 under different conditions in the membrane. Here we did not observe an immersed I-state, which would have been expected to correspond to an upright transmembrane helix that is compatible with a pore. These differences between the two models and the open questions concerning the parallel versus antiparallel nature of the dimer and its alignment in a transmembrane pore may be related to the different experimental conditions under which the REDOR experiments and the oriented measurements were carried out. Distance constraints had to be collected in frozen or lyophilized bilayer samples, whereas the orientational constraints were acquired under quasi-native conditions in liquid crystalline DMPC at 35 °C. It is thus conceivable that some of the apparent contradictions may be reconciled once the MSI-103 samples are prepared and observed under exactly the same conditions. Unfortunately, it is not possible to collect meaningful REDOR constraints in liquid crystalline samples, and an orientational analysis in frozen or lyophilized bilayers is not considered to be biologically relevant. At present, the parallel or antiparallel nature of the proposed dimers is an unresolved question, and it is possible that different types of dimers form under different conditions. Overall, in the study of membrane-active peptides, it is essential to realize that their structural and dynamic behavior may depend dramatically on subtle changes in peptide concentration, sample hydration, lipid composition, temperature, etc. (*17*, *18*, *22*, *29*, *48*, *52*).

Structure−Function Relationship. All mutant MSI-103 peptides, in which Ala-d_3 was substituted for Ile or Gly, or in which CF_3-Phg was introduced, have been characterized in terms their antimicrobial activity. Using a 2-fold dilution series, it is not possible to state exact values of MIC, and a slight change in activity can give rise to a factor of 2 in the apparent result. Thus, for a difference to be significant, the MICs should differ by a factor of at least 4. In most cases, we found that the mutants have the same MIC as wild-type MSI-103. When Gly was replaced with Ala-d_3, no effect was seen, and likewise, when Ile was replaced with CF_3-Phg, the MIC did not change. In these mutants, the size and polarity of the side chain were not significantly altered. Also, when Ile was replaced with Ala-d_3, no effect was seen (except for MSI-I9-^{19}F which was slightly less active against *B. subtilis*), indicating that even the change from a large to a small side chain was readily accommodated. Only MSI-G11-^{19}F shows a much lower activity against most of the bacteria that were tested. This is the mutant which suffers the largest difference compared to the wild type, as Gly is replaced with a bulky CF_3-Phg side chain. On the other hand, when the small Ala at position 10 was replaced with CF_3-Phg, no effect was seen, except for a slightly reduced activity against *Acinetobacter* sp (DSM 586). It is therefore possible that the strong effect at position Gly11 is not so much due to a general effect of side chain volume as rather to some more specific importance of this site (see below). For PGLa, it has been reported previously that the antimicrobial effect was not affected by introduction of CF_3-Phg at various positions, except that a weaker effect was observed when Ala8 was mutated, which is located on the hydrophilic face of the peptide and thus would expose the large and hydrophobic CF_3-Phg to the aqueous surface (*13*).

In contrast to the antimicrobial tests, the hemolysis assays showed that mutations had large effects on the ability of peptides to lyse erythrocyte ghosts. Some mutations almost completely abolished hemolysis, while others increased the activity of the peptide significantly. Most remarkable was the reduction of activity when Ile9 or Ile13 was replaced with Ala-d_3, whereas a substitution of Ala10 or Gly9 with CF_3-Phg led to a considerable increase. We thus conclude that the hemolytic response correlates directly with the change in hydrophobicity of the peptides, which has been previously identified as an important factor (*53*−*55*). Changing Ile to CF_3-Phg or Gly to Ala-d_3 gave a much weaker effect, as the hydrophobicity did not change much with these mutations, though the same trend is seen even in these cases. In Table 9, the relationship between the hydrophobicity and hemolytic activity of the various MSI-103 analogues is illustrated. We have previously observed a decrease in hemolytic activity upon removal of the C-terminal amide group of MSI-103 and related peptides (*26*), which may indeed be explained by the lower hydrophobicity once the charged carboxyl group is introduced at the free C-terminus. Overall, it is remarkable that the strong dependence of hemolytic activity on particular mutations does not seem to be related to the antimicrobial activity. Since the antimicrobial function occurs at much lower peptide concentrations and is largely insensitive to mutations, it seems likely that different mechanisms are involved in these two membrane-perturbing processes.

With regard to the biological effects of the original peptides, MSI-103 had been specifically designed to be a better antibiotic than PGLa (*3*, *25*, *26*). We have concluded from this work that MSI-103 can dimerize in a manner similar to that of PGLa, but at a lower threshold, and MSI-103 also starts to form immobilized assemblies in the bilayer at a lower concentration than PGLa. The stronger propensity of MSI-103 to dimerize and form higher-order oligomers thus appears to be correlated with its higher antimicrobial activity.

ACKNOWLEDGMENT

We are grateful to Silvia Gehrlein and Stefanie Maurer at Forschungszentrum Karlsruhe for help with peptide synthesis and purification. We also thank Marco Ieronimo for help with hemolysis assays, Marina Berditsch for help with antimicrobial assays, Pierre Tremouilhac for help with Figure 1, and Jake Schaefer for constructive discussions.

SUPPORTING INFORMATION AVAILABLE

Analysis of ^{19}F NMR data using helix model A. This material is available free of charge via the Internet at http://pubs.acs.org.

REFERENCES

1. Boman, H. G. (2003) Antibacterial peptides: Basic facts and emerging concepts, *J. Intern. Med. 254*, 197−215.

2. Hancock, R. E., and Chapple, D. S. (1999) Peptide antibiotics, *Antimicrob. Agents Chemother. 43*, 1317−1323.
3. Maloy, W. L., and Kari, U. P. (1995) Structure-activity studies on magainins and other host defense peptides, *Biopolymers 37*, 105−122.
4. Reddy, K. V., Yedery, R. D., and Aranha, C. (2004) Antimicrobial peptides: Premises and promises, *Int. J. Antimicrob. Agents 24*, 536−547.
5. Brogden, K. A. (2005) Antimicrobial peptides: Pore formers or metabolic inhibitors in bacteria? *Nat. Rev. Microbiol. 3*, 238−250.
6. Zasloff, M. (1987) Magainins, a class of antimicrobial peptides from Xenopus skin: Isolation, characterization of two active forms, and partial cDNA sequence of a precursor, *Proc. Natl. Acad. Sci. U.S.A. 84*, 5449−5453.
7. Wade, D., Boman, A., Wahlin, B., Drain, C. M., Andreu, D., Boman, H. G., and Merrifield, R. B. (1990) All-D amino acid-containing channel-forming antibiotic peptides, *Proc. Natl. Acad. Sci. U.S.A. 87*, 4761−4765.
8. Hoffmann, W., Richter, K., and Kreil, G. (1983) A novel peptide designated PYLa and its precursor as predicted from cloned mRNA of *Xenopus laevis* skin, *EMBO J. 2*, 711−714.
9. Andreu, D., Aschauer, H., Kreil, G., and Merrifield, R. B. (1985) Solid-phase synthesis of PYLa and isolation of its natural counterpart, PGLa [PYLa-(4−24)] from skin secretion of *Xenopus laevis*, *Eur. J. Biochem. 149*, 531−535.
10. Gibson, B. W., Poulter, L., Williams, D. H., and Maggio, J. E. (1986) Novel peptide fragments originating from PGLa and the cerulein and xenopsin precursors from *Xenopus laevis*, *J. Biol. Chem. 261*, 5341−5349.
11. Latal, A., Degovics, G., Epand, R. F., Epand, R. M., and Lohner, K. (1997) Structural aspects of the interaction of peptidyl-glycylleucine-carboxyamide, a highly potent antimicrobial peptide from frog skin, with lipids, *Eur. J. Biochem. 248*, 938−946.
12. Wieprecht, T., Apostolov, O., Beyermann, M., and Seelig, J. (2000) Membrane binding and pore formation of the antibacterial peptide PGLa: Thermodynamic and mechanistic aspects, *Biochemistry 39*, 442−452.
13. Glaser, R. W., Sachse, C., Dürr, U. H. N., Wadhwani, P., and Ulrich, A. S. (2004) Orientation of the antimicrobial peptide PGLa in lipid membranes determined from ^{19}F-NMR dipolar couplings of 4-CF_3-phenylglycine labels, *J. Magn. Reson. 168*, 153−163.
14. Bechinger, B., Zasloff, M., and Opella, S. J. (1998) Structure and dynamics of the antibiotic peptide PGLa in membranes by solution and solid-state nuclear magnetic resonance spectroscopy, *Biophys. J. 74*, 981−987.
15. Strandberg, E., and Ulrich, A. S. (2004) NMR methods for studying membrane-active antimicrobial peptides, *Concepts Magn. Reson., Part A 23*, 89−120.
16. Ulrich, A. S., Wadhwani, P., Dürr, U. H. N., Afonin, S., Glaser, R. W., Strandberg, E., Tremouilhac, P., Sachse, C., Berditchevskaia, M., and Grage, S. L. (2006) Solid-state ^{19}F-nuclear magnetic resonance analysis of membrane-active peptides, in *NMR spectroscopy of biological solids* (Ramamoorthy, A., Ed.) pp 215−236, CRC Press, Boca Raton, FL.
17. Glaser, R. W., Sachse, C., Dürr, U. H. N., Afonin, S., Wadhwani, P., Strandberg, E., and Ulrich, A. S. (2005) Concentration-dependent realignment of the antimicrobial peptide PGLa in lipid membranes observed by solid-state ^{19}F-NMR, *Biophys. J. 88*, 3392−3397.
18. Strandberg, E., Wadhwani, P., Tremouilhac, P., Dürr, U. H. N., and Ulrich, A. S. (2006) Solid-state NMR analysis of the PGLa peptide orientation in DMPC bilayers: Structural fidelity of ^{2}H-labels versus high sensitivity of ^{19}F-NMR, *Biophys. J. 90*, 1676−1686.
19. Wakamatsu, K., Takeda, A., Tachi, T., and Matsuzaki, K. (2002) Dimer structure of magainin 2 bound to phospholipid vesicles, *Biopolymers 64*, 314−327.
20. Toke, O., Maloy, W. L., Kim, S. J., Blazyk, J., and Schaefer, J. (2004) Secondary structure and lipid contact of a peptide antibiotic in phospholipid bilayers by REDOR, *Biophys. J. 87*, 662−674.
21. Toke, O., O'Connor, R. D., Weldeghiorghis, T. K., Maloy, W. L., Glaser, R. W., Ulrich, A. S., and Schaefer, J. (2004) Structure of $(KIAGKIA)_3$ aggregates in phospholipid bilayers by solid-state NMR, *Biophys. J. 87*, 675−687.
22. Tremouilhac, P., Strandberg, E., Wadhwani, P., and Ulrich, A. S. (2006) Conditions affecting the re-alignment of the antimicrobial peptide PGLa in membranes as monitored by solid state ^{2}H-NMR, *Biochim. Biophys. Acta 1758*, 1330−1342.
23. Tremouilhac, P., Strandberg, E., Wadhwani, P., and Ulrich, A. S. (2006) Synergistic transmembrane alignment of the antimicrobial heterodimer PGLa/magainin, *J. Biol. Chem. 281*, 32089−32094.
24. Zelezetsky, I., Pag, U., Sahl, H. G., and Tossi, A. (2005) Tuning the biological properties of amphipathic α-helical antimicrobial peptides: Rational use of minimal amino acid substitutions, *Peptides 26*, 2368−2376.
25. Blazyk, J., Wiegand, R., Klein, J., Hammer, J., Epand, R. M., Epand, R. F., Maloy, W. L., and Kari, U. P. (2001) A novel linear amphipathic β-sheet cationic antimicrobial peptide with enhanced selectivity for bacterial lipids, *J. Biol. Chem. 276*, 27899−27906.
26. Strandberg, E., Tiltak, D., Ieronimo, M., Kanithasen, N., Wadhwani, P., and Ulrich, A. S. (2007) Influence of C-terminal amidation on the antimicrobial and hemolytic activities of cationic α-helical peptides, *Pure Appl. Chem. 79*, 717−728.
27. Afonin, S., Glaser, R. W., Berditchevskaia, M., Wadhwani, P., Guhrs, K. H., Mollmann, U., Perner, A., and Ulrich, A. S. (2003) 4-Fluorophenylglycine as a label for ^{19}F-NMR structure analysis of membrane-associated peptides, *ChemBioChem 4*, 1151−1163.
28. Bürck, J., Wadhwani, P., Afonin, S., Strandberg, E., and Ulrich, A. S. (2007) manuscript to be submitted for publication.
29. Chen, F. Y., Lee, M. T., and Huang, H. W. (2002) Sigmoidal concentration dependence of antimicrobial peptide activities: A case study on alamethicin, *Biophys. J. 82*, 908−914.
30. Ludtke, S., He, K., and Huang, H. (1995) Membrane thinning caused by magainin 2, *Biochemistry 34*, 16764−16769.
31. Rance, M., and Byrd, R. A. (1983) Obtaining high-fidelity spin-1/2 powder spectra in anisotropic media: Phase-cycled Hahn echo spectroscopy, *J. Magn. Reson. 52*, 221−240.
32. Davis, J. H., Jeffrey, K. R., Bloom, M., Valic, M. I., and Higgs, T. P. (1976) Quadrupolar echo deuteron magnetic resonance spectroscopy in ordered hydrocarbon chains, *Chem. Phys. Lett. 42*, 390−394.
33. Zhang, S., Wu, X. L., and Mehring, M. (1990) Elimination of ringing effects in multiple-pulse sequences, *Chem. Phys. Lett. 173*, 481−484.
34. Bennett, A. E., Rienstra, C. M., Auger, M., Lakshmi, K. V., and Griffin, R. G. (1995) Heteronuclear decoupling in rotating solids, *J. Chem. Phys. 103*, 6951−6958.
35. Salgado, J., Grage, S. L., Kondejewski, L. H., Hodges, R. S., McElhaney, R. N., and Ulrich, A. S. (2001) Membrane-bound structure and alignment of the antimicrobial β-sheet peptide gramicidin S derived from angular and distance constraints by solid state ^{19}F-NMR, *J. Biomol. NMR 21*, 191−208.
36. Van der Wel, P. C. A., Strandberg, E., Killian, J. A., and Koeppe, R. E., II (2002) Geometry and intrinsic tilt of a tryptophan-anchored transmembrane α-helix determined by ^{2}H NMR, *Biophys. J. 83*, 1479−1488.
37. Afonin, S., Dürr, U. H. N., Glaser, R. W., and Ulrich, A. S. (2004) 'Boomerang'-like insertion of a fusogenic peptide in a lipid membrane revealed by solid-state ^{19}F-NMR, *Magn. Reson. Chem. 42*, 195−203.
38. Strandberg, E., Özdirekcan, S., Rijkers, D. T. S., Van der Wel, P. C. A., Koeppe, R. E., II, Liskamp, R. M. J., and Killian, J. A. (2004) Tilt angles of transmembrane model peptides in oriented and non-oriented lipid bilayers as determined by ^{2}H solid state NMR, *Biophys. J. 86*, 3709−3721.
39. Ulrich, A. S. (2005) Solid state ^{19}F-NMR methods for studying biomembranes, *Prog. Nucl. Magn. Reson. Spectrosc. 46*, 1−21.
40. Afonin, S., Mikhailiuk, P. K., Komarov, I. V., and Ulrich, A. S. (2007) Evaluating the amino acid CF_3-bicyclopentylglycine as a new label for solid-state ^{19}F-NMR structure analysis of membrane-bound peptides, *J. Pept. Sci. 13*, 614−623.
41. Ulrich, A. S., Heyn, M. P., and Watts, A. (1992) Structure determination of the cyclohexene ring of retinal in bacteriorhodopsin by solid-state deuterium NMR, *Biochemistry 31*, 10390−10399.
42. Ulrich, A. S., and Watts, A. (1993) ^{2}H NMR lineshapes of immobilized uniaxially oriented membrane proteins, *Solid State Nucl. Magn. Reson. 2*, 21−36.
43. Ulrich, A. S., Watts, A., Wallat, I., and Heyn, M. P. (1994) Distorted structure of the retinal chromophore in bacteriorhodopsin resolved by ^{2}H-NMR, *Biochemistry 33*, 5370−5375.
44. Ulrich, A. S., Wallat, I., Heyn, M. P., and Watts, A. (1995) Re-alignment of the retinal chromophore in the M-photointermediate of bacteriorhodopsin, *Nat. Struct. Biol. 2*, 190−192.
45. Davis, J. H. (1983) The description of membrane lipid conformation, order and dynamics by ^{2}H-NMR, *Biochim. Biophys. Acta 737*, 117−171.

46. Huang, H. W. (2006) Molecular mechanism of antimicrobial peptides: The origin of cooperativity, *Biochim. Biophys. Acta 1758*, 1292−1302.
47. Wu, Y., Huang, H. W., and Olah, G. A. (1990) Method of oriented circular dichroism, *Biophys. J. 57*, 797−806.
48. Huang, H. W., and Wu, Y. (1991) Lipid-alamethicin interactions influence alamethicin orientation, *Biophys. J. 60*, 1079−1087.
49. Hara, T., Mitani, Y., Tanaka, K., Uematsu, N., Takakura, A., Tachi, T., Kodama, H., Kondo, M., Mori, H., Otaka, A., Nobutaka, F., and Matsuzaki, K. (2001) Heterodimer formation between the antimicrobial peptides magainin 2 and PGLa in lipid bilayers: A cross-linking study, *Biochemistry 40*, 12395−12399.
50. Matsuzaki, K., Murase, O., Tokuda, H., Funakoshi, S., Fujii, N., and Miyajima, K. (1994) Orientational and aggregational states of magainin 2 in phospholipid bilayers, *Biochemistry 33*, 3342−3349.
51. Hristova, K., Dempsey, C. E., and White, S. H. (2001) Structure, location, and lipid perturbations of melittin at the membrane interface, *Biophys. J. 80*, 801−811.
52. Ludtke, S. J., He, K., Wu, Y. L., and Huang, H. W. (1994) Cooperative membrane insertion of magainin correlated with its cytolytic activity, *Biochim. Biophys. Acta 1190*, 181−184.
53. Dathe, M., Wieprecht, T., Nikolenko, H., Handel, L., Maloy, W. L., MacDonald, D. L., Beyermann, M., and Bienert, M. (1997) Hydrophobicity, hydrophobic moment and angle subtended by charged residues modulate antibacterial and haemolytic activity of amphipathic helical peptides, *FEBS Lett. 403*, 208−212.
54. Kondejewski, L. H., Jelokhani-Niaraki, M., Farmer, S. W., Lix, B., Kay, C. M., Sykes, B. D., Hancock, R. E., and Hodges, R. S. (1999) Dissociation of antimicrobial and hemolytic activities in cyclic peptide diastereomers by systematic alterations in amphipathicity, *J. Biol. Chem. 274*, 13181−13192.
55. Chen, Y., Mant, C. T., Farmer, S. W., Hancock, R. E., Vasil, M. L., and Hodges, R. S. (2005) Rational design of α-helical antimicrobial peptides with enhanced activities and specificity/therapeutic index, *J. Biol. Chem. 280*, 12316−12329.

BI701944R